




Open Archive Toulouse Archive Ouverte (OATAO)

OATAO is an open access repository that collects the work of Toulouse researchers and makes it freely available over the web where possible

This is an author's version published in: <http://oatao.univ-toulouse.fr/21043>



Official URL: <https://doi.org/10.1111/srt.12643>

To cite this version:

Villaret, Aurélie and Ipinazar, Célia and Satar, Tuvana and Gravier, Eléonore and Mias, Céline and Questel, Emmanuel and Schmitt, Anne-Marie and Samouillan, Valérie  and Nadal-Wollbold, Florence and Josse, Gwendal *Raman characterization of human skin aging*. (In Press: 2018) *Skin Research and Technology*. ISSN 0909-752X

Any correspondence concerning this service should be sent to the repository administrator: tech-oatao@listes-diff.inp-toulouse.fr

Raman characterization of human skin aging

Aurélie Villaret¹  | Célia Ipinazar¹ | Tuvana Satar¹ | Eléonore Gravier¹ |
Céline Mias¹  | Emmanuel Questel¹ | Anne-Marie Schmitt¹ | Valérie Samouillan²  |
Florence Nadal¹ | Gwendal Josse¹ 

¹Centre de Recherche sur la Peau, Pierre Fabre Dermo-Cosmétique, Toulouse, France

²CIRIMAT UMR 5085, Institut Carnot, Equipe Physique des Polymères, Paul Sabatier University, Toulouse Cedex, France

Correspondence

Aurélie Villaret, Pierre Fabre Dermo-Cosmétique, Hôtel Dieu Saint Jacques, Toulouse Cedex 3, France.
Email: aurelie.villaret.externe@pierre-fabre.com

Abstract

Background: Skin aging is a complex biological process mixing intrinsic and extrinsic factors, such as sun exposure. At the molecular level, skin aging affects in particular the extracellular matrix proteins.

Materials and Methods: Using Raman imaging, which is a nondestructive approach appropriate for studying biological samples, we analyzed how aging modifies the matrix proteins of the papillary and reticular dermis. Biopsies from the buttock and dorsal forearm of volunteers younger than 30 and older than 60 were analyzed in order to identify chronological and photoaging processes. Analyses were performed on skin section, and Raman spectra were acquired separately on the different dermal layers.

Results: We observed differences in dermal matrix structure and hydration state with skin aging. Chronological aging alters in particular the collagen of the papillary dermis, while photoaging causes a decrease in collagen stability by altering proline and hydroxyproline residues in the reticular dermis. Moreover, chronological aging alters glycosaminoglycan content in both dermal compartments.

Conclusion: Alterations of the papillary and reticular dermal matrix structures during photo- and chronological aging were clearly depicted by Raman spectroscopy.

KEYWORDS

collagen, dermis, glycosaminoglycan, hydration state, hydroxyproline, proline, Raman spectroscopy

1 | INTRODUCTION

Skin aging is a physiological process that also involves biochemical, structural, and functional changes. As life expectancy increases, there is a growing need to gain better understanding of the molecular mechanisms of skin aging. This process is driven not only by endogenous mechanisms but also by exogenous factors such as solar exposure.

The functional properties of the skin are greatly affected by aging, leading to poor mechanical properties and fragility.¹ The skin's mechanical properties are mainly controlled by the dermal

architecture, and for this reason, the structure of the dermis has been widely analyzed.

The dermis is a connective tissue containing high levels of extracellular matrix proteins, mainly collagens, elastin, and glycosaminoglycan (GAG). Collagen I, which represents around 90% of collagen fibrils, decreases with aging, due to a lower synthesis level and a higher matrix degradation.²⁻⁴ Collagen degradation can be caused either by direct UV absorption or through matrix metalloproteinase activities.¹ Differences between photoaging and chronological aging have been observed on collagen fibers' structure: These fibers are thickened and fragmented on photo-exposed areas,⁵ while they appear more stable on skin subjected only to chronological aging.^{2,6}

Another feature of photoaging is the increase of GAG proportion in the dermis.^{7,8}

Skin aging is also associated with changes in water level in the dermis. Water molecules in biological tissue are either bounded to proteins or in bulk state (also called "free water"). Bound water plays a crucial role in maintaining the structural properties of proteins. The structural stability of collagen is controlled by hydrogen bonds established between amino acid residues and water molecules.^{9,10} Indeed, hydroxyproline residues maintain the hydration networks by linking the adjacent triple helices of the collagen fibrils.^{11,12} Moreover, the collagen's hydration level controls the fiber bundles' compactness, which has been described as decreasing with age.¹⁰ In young skin, water is essentially observed in bounded form,¹³ while in photoaged skin the water-protein interactions decrease.^{2,14} This phenomenon leads to an alteration of the overall protein stability.⁵ Moreover, in skin aging, the free water content of the dermis increases,² principally in the papillary dermis.^{14,15}

Raman spectroscopy is a noninvasive and nondestructive optical method used for obtaining molecular fingerprints of biological samples. It is based on light-tissue interaction, which enables the analysis of the molecule's vibrational modes. Interestingly, identification of Raman spectral bands for collagen has already been performed by several teams.¹⁶⁻¹⁸ This is a very suitable technique for determining molecular and structural modifications occurring during biological process such as skin aging.^{10,14,15,19,20} Gniadecka et al studied the water and protein structure in photoaged and chronically aged skin. They observed a decrease in amide III band intensity in the photoaged skin showing a change in the protein conformational structure.¹⁴ In a previous work, using Fourier transform infrared (FTIR) spectroscopy and thermal analysis, we highlighted the difference between chronological and photoinduced skin aging.² In the present study, we show that Raman spectroscopy brings precise information on the collagen structure of the dermis.

2 | MATERIALS AND METHODS

2.1 | Volunteers

Seven healthy young women (age range 20-30 years old) and seven healthy older women (age > 60 years old) presenting clinical signs of photoaging (SCINEXA, SCore for INtrinsic and EXtrinsic skin Aging, score ≥ 2) were enrolled after they had provided written informed consent. SCINEXA is a score which grades intrinsic (<2) and extrinsic (≥ 2) aging.²¹

The clinical study was carried out at the Pierre Fabre Skin Research Centre, Toulouse, France, in accordance with the ethical principles of the Declaration of Helsinki. The protocol was approved by the Southwest Ethics Committee and Overseas III in Bordeaux, France (VIEILBIOCLIDERM), and by the French Agency for the Safety of Health Products (ID RCB 2017-A00698-39, ANSM).

2.2 | Skin samples

Four-millimeter punch biopsies were taken from each subject on sun-protected buttock and sun-exposed dorsal forearm skin. Samples were immediately embedded into OCT (optimal cutting temperature) compound and frozen in liquid nitrogen. Thin (10 μm) longitudinal cross sections were deposited on CaF₂ windows and analyzed with Raman spectroscopy in imaging mode. No sample pre-treatment was performed. For each sample, the delimitation between the papillary and reticular dermis was visualized from dark-field microscopic images.

2.3 | Confocal Raman microspectrometer measurements

Raman data were collected with an optical fiber BX-FM microscope (Olympus, Tokyo, Japan) coupled with an iHR320 spectrometer equipped with a Peltier-cooled CCD detector (Horiba Jobin Yvon, Villeneuve d'Ascq, France). A 660-nm laser diode was used as an excitation source. The incident laser beam was focused on the sample using a 100 \times objective lens (NA = 0.9, Olympus). The Raman scattering signal was collected through a confocal pinhole of 100 μm . The laser power on the sample was 26 mW. The collected light was dispersed using a holographic grating of 600 lines/mm. The data were collected on a spectral range from 400 to 1800 cm^{-1} with a spectral resolution of 2.8 cm^{-1} . Spectral images were acquired using a motorized stage in point-by-point mode. A step size of 20 μm was used on the x-axis (parallel to skin surface). On the y-axis, a step size of 4 μm in the papillary and 5 μm in the reticular dermis was used. To compare the intensity of bands in the region of 400-1800 cm^{-1} , spectra were normalized with the 1004 cm^{-1} band relative to phenylalanine. No smoothing procedures were used.

2.4 | Statistical analysis

For each peak, a linear mixed model was fitted to estimate the differences of Raman measurements between groups (young/older) by site (forearm/buttock). The factors "group," "site," and the interaction "group/site" were considered as fixed factors. The factor "subject" was considered as a random factor. Pairwise differences of least square means for the interaction term were then computed and tested. *P*-values were based on the t-distribution using degrees of freedom computed with the Satterthwaite method. *P* values under 5% were considered significant. The R software v3.3.1 was used for statistical analyses (The R Project for Statistical Computing [<http://www.cran.r-project.org/>]).

3 | RESULTS

3.1 | Optical microscopy

Images and Raman spectra from the papillary and reticular dermis of young (Y) and aged (A) skin samples taken from photo-protected (P) and photo-exposed (E) body sites are presented in Figure 1. Optical microscopy images (in dark-field mode) were taken on each

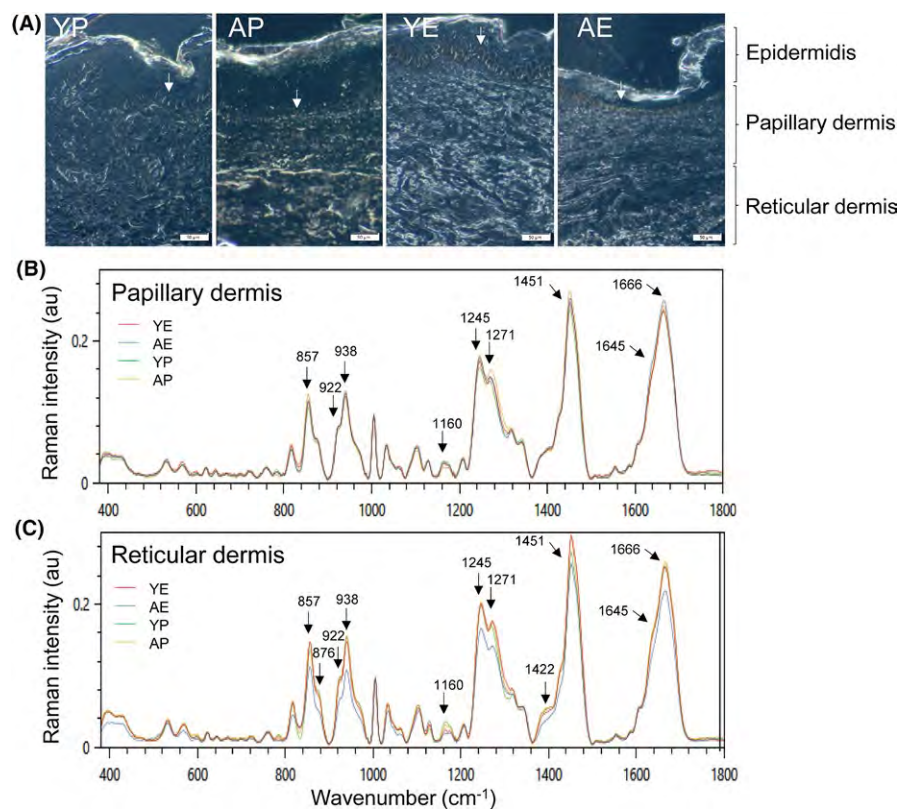


FIGURE 1 Optical microscopy—Raman spectra. (A) Representative cross-sectional microscopic images of human skin sections of young and aged subjects on sun-protected (buttock) and sun-exposed (dorsal forearm) sites. The white arrows indicate the dermo-epidermal junction. Scale bars of 50 μm . Average Raman spectra ($n = 7$) of papillary (B) and reticular (C) dermis in sun-protected buttock skin and sun-exposed dorsal forearm skin from young and aged individuals. All spectra were normalized with phenylalanine ($995\text{--}1015\text{ cm}^{-1}$). A, aged; au, arbitrary units; E, exposed; P, protected; Y, young. YE, red spectra; AE, blue spectra; YP, green spectra; AP, yellow spectra

sample in order to determine the positions of the papillary and reticular dermis (Figure 1A). Visual inspection of the images from the different skin sites and groups was performed. For both skin sites, we observed a decrease with aging of the dermo-epidermal junction thickness (Figure 1A, arrows). Moreover, the fibers appeared less organized and less dense in the aged skin samples (Figure 1A).

3.2 | Full Raman spectra

Raman spectroscopy was used to determine the molecular fingerprint of the different samples at different depth. For the papillary dermis, only small differences between the two age groups' average Raman spectra could be visualized (Figure 1B). Nevertheless, AP spectra were different from the spectra of the other samples (YP, YE, and AE). On the reticular dermis, much larger difference in Raman spectra was measured between the two age groups (Figure 1C). Raman spectra were analyzed in order to identify glycosaminoglycan and the two main matrix skin components, which are collagen and elastin.^{16,22}

3.3 | Analysis of papillary dermis matrix

A significant increase of the CH bending mode of collagen at 1451 cm^{-1} was observed on the AP samples comparing to the YP samples (Figure 2D). Scattering modes $\nu(\text{C-C})$ of proline residues at 857 cm^{-1} were also observed larger in the AP samples compared to YP samples (Figure 2B). Moreover, the proline-poor/proline-rich ratio ($1245/1271\text{ cm}^{-1}$) was significantly lower in the AP samples (Figure 2C).

Vibratory modes relative to hydrogen bonds between carbonyl groups of proline and hydroxyproline residues of collagen and water molecules were measured at 938 cm^{-1} .^{9,10,23} The $938/922$ ratio was significantly lower for the AP samples (Figure 2A), indicating a decrease in collagen hydration state.¹⁰ This later observation showed that the papillary dermis hydration state is modified during chronological aging. But on the photo-exposed papillary dermis, no clear changes between age groups in the matrix structure were observed.

3.4 | Analysis of reticular dermis matrix

Raman measurements in the reticular dermis showed significantly lower signals for all the peaks related to proline and hydroxyproline residues of collagen ($857, 876, 938, 1245, \text{ and } 1271\text{ cm}^{-1}$)¹⁸ on the AE samples (Figure 3) comparing to the YE samples. Constitutive amino acids of collagen have a strong Raman scattering due to their aromatic rings, visualized at 1422 cm^{-1} (carboxyl groups of aspartate and glutamate).¹⁷ Interestingly, this peak was significantly decreased on the AE reticular dermal samples compared to YE samples confirming a structural alteration of the collagen structure or a decrease of collagen content (Figure 3).

We observed that collagen alterations occurring during photo-aging are associated with lower signals of the proline and hydroxyproline residues in reticular dermis. But on the photo-protected reticular derma, no clear changes between age groups in the matrix structure were observed.

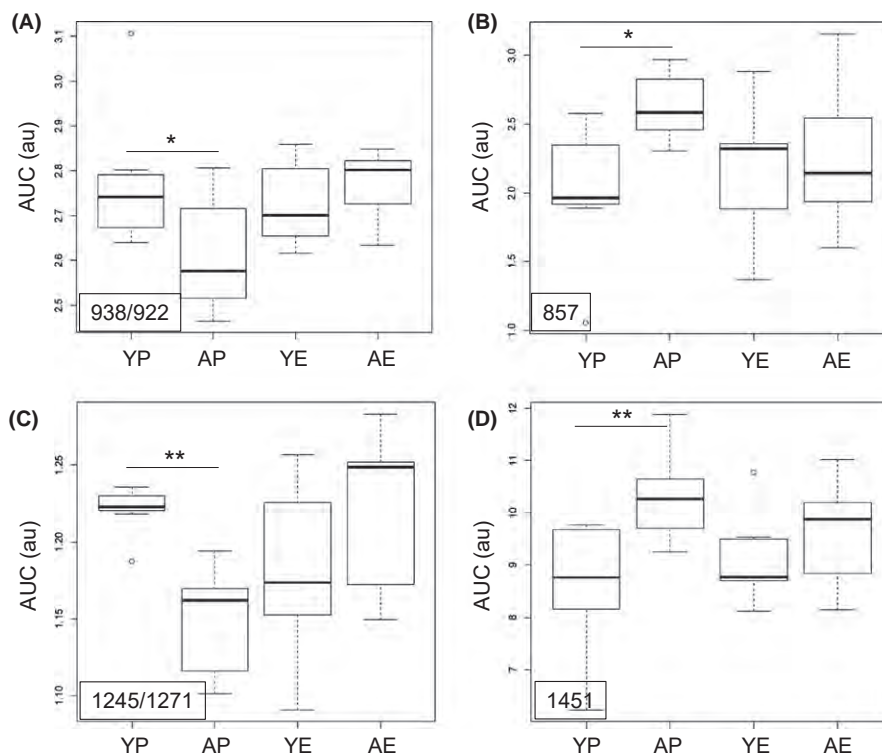


FIGURE 2 Raman spectroscopy analysis of collagen structure in the papillary dermis during chronological aging. Mean area values of peaks relative to collagen structure: A, 938/922 cm^{-1} ; B, 857 cm^{-1} ; C, 1245/1271 cm^{-1} ; and D, 1451 cm^{-1} . All spectra were normalized with phenylalanine (995-1015 cm^{-1}). A, aged; au, arbitrary units; AUC, area under curve; E, exposed; P, protected; Y, young. Data are visualized using boxplots. The black line represents the AUC median values. The bottom and top of the boxes represent the 25th and 75th percentile, respectively, whereas the box represents the interquartile range. The whiskers extend to the most extreme data point which is no more than 1.5 times the interquartile range from the box. The points at the top (respectively bottom) of the boxplots represent the maximum (respectively minimum) AUC value. * $P < 0.05$, ** $P < 0.01$, *** $P < 0.001$, linear mixed model

3.5 | Elastin

No modification between the two age groups was observed for the 722 cm^{-1} band relative to elastin²⁴ (data not shown).

3.6 | Glycosaminoglycan content

For both papillary and reticular dermal areas, the 1160 cm^{-1} band, which is attributed to glycosaminoglycan Raman scattering,^{10,22} appeared with a significantly lower signal for AP samples compared to YP samples (Figure 4A,B).

4 | DISCUSSION

In this study, changes in dermal structure during chronological and photoaging were measured by Raman spectroscopy. Raman analyses without staining were performed on transverse skin section in order to analyze the papillary and the reticular dermis separately.

The analysis showed that collagen structure in papillary dermis was modified during chronological aging. First, we observed a higher CH bending mode at 1451 cm^{-1} for AP compared to YP subjects on the papillary dermis. This vibrational signature takes place outside

the protein chain and does not strongly participate in intermolecular interactions.^{14,16} In our previous study,² thermal analysis highlighted an increase of heat-stable crosslinks in response to chronological aging, which could reflect oxidation mechanisms such as age-induced glycation products and/or carbonyl changes.²⁵ However, in a *in vitro* model the Raman band at 1451 cm^{-1} was described as remaining constant upon glycation of type I collagen.²⁶

On the papillary dermis, we also observed that chronological aging was associated with a decrease of the 938/922 ratio. This result is in agreement with a recent study performed *in vivo* on the papillary dermis, where de Vasconcelos Nasser Caetano et al¹⁹ attributed the reduction of the 855 cm^{-1} and 938 cm^{-1} band intensities to collagen alterations during intrinsic aging. Zhang et al showed that the 938 cm^{-1} band provides a measurement of the collagen highly bonded with water.⁹ Xiao et al²³ studied the effect of environmental changes (temperature, salt concentration) on the *trans*-to-*cis* proline and hydroxyproline isomerization. They demonstrated that the 938 cm^{-1} peak was also a good indicator of *trans*-to-*cis* isomerization changes in proline and hydroxyproline residues in collagen.²³ Nguyen et al studied the water content in skin in samples from different age groups by calculating the two ratios 938/922 and 1658/1668 cm^{-1} .¹² They observed an upward trend for 938/922 cm^{-1} ratio and a significant increase of the

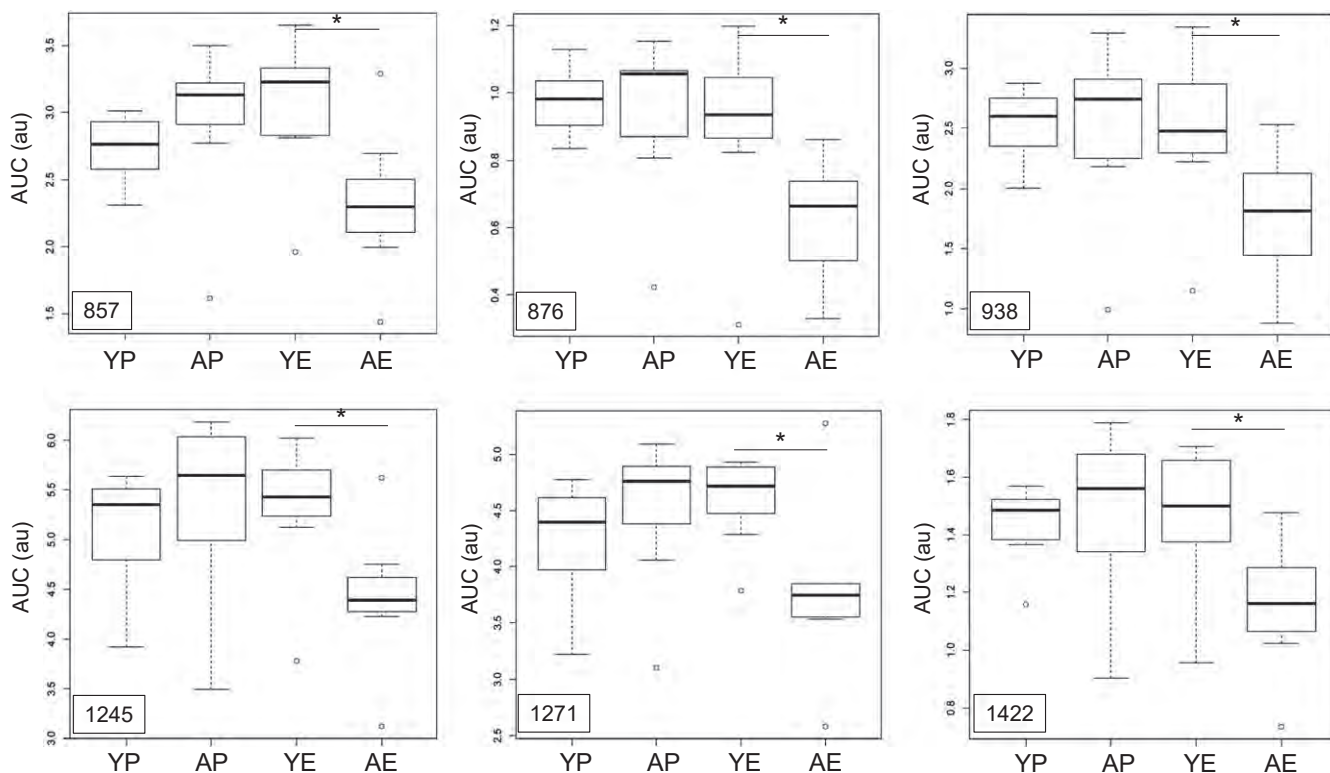


FIGURE 3 Raman spectroscopy analysis of photoaging on reticular dermis. Mean area values of peaks relative to collagen structure. All spectra were normalized with phenylalanine ($995\text{-}1015\text{ cm}^{-1}$). A, aged; au, arbitrary units; AUC, area under curve; E, exposed; P, protected; Y, young. Data are visualized using boxplots. The black line represents the AUC median values. The bottom and top of the boxes represent the 25th and 75th percentile, respectively, whereas the box represents the interquartile range. The whiskers extend to the most extreme data point which is no more than 1.5 times the interquartile range from the box. The points at the top (respectively, bottom) of the boxplots represent the maximum (respectively, minimum) AUC value. * $P < 0.05$, ** $P < 0.01$, *** $P < 0.001$, linear mixed model

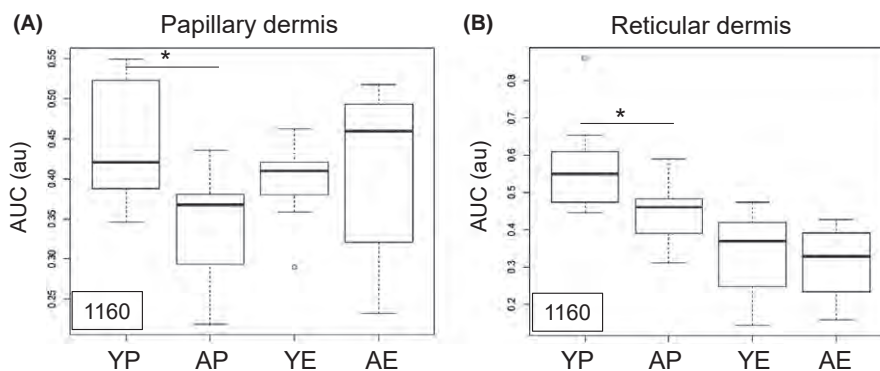


FIGURE 4 Raman spectroscopy analysis of skin glycosaminoglycan content. Mean value of glycosaminoglycan content for the different samples (band area in the range $1150\text{-}1170\text{ cm}^{-1}$) in the papillary (A) and in the reticular (B) dermis. A, aged; au, arbitrary units; AUC, area under curve; E, exposed; P, protected; Y, young. All spectra were normalized with phenylalanine ($995\text{-}1015\text{ cm}^{-1}$). Data are visualized using boxplots. The black line represents the AUC median values. The bottom and the top of the boxes represent the 25th and 75th percentile, respectively, whereas the box represents the interquartile range. The whiskers extend to the most extreme data point which is no more than 1.5 times the interquartile range from the box. The points at the top (respectively, bottom) of the boxplots represent the maximum (respectively, minimum) AUC value. * $P < 0.05$, ** $P < 0.01$, *** $P < 0.001$, linear mixed model

$1658/1668\text{ cm}^{-1}$ ratio in the older skin sample, proving that collagen fiber compactness decreases during skin aging.

Our observations tend to show that during chronological aging, collagen hydration and fiber compactness diminish. This reduced

compactness probably results from *trans*-to-*cis* isomerization of proline and hydroxyproline residues in the collagen molecules. Moreover, we also observed a decrease in glycosaminoglycan content as demonstrated by Oh et al²⁷ with biochemical methods.

Previous studies investigated changes in fiber orientation with chronological aging. Using polarized FTIR microimaging, Eklouh et al²⁸ showed that in young subjects, collagen fibers are mostly oriented perpendicularly to the skin surface, whereas in aged skin, samples fibers are highly parallel to it, principally in the papillary dermis. Using Raman spectroscopy, conformational changes in the dermal collagen between normal and peri-tumoral tissue were measured through the 1245/1271 ratio.²⁹ Similar results have also been reported by Short et al,³⁰ who interpreted these observations as a degradation of collagen into gelatin.

Furthermore, we observed in the present study that photoaging has a strong impact on the collagen structure of the reticular dermis. Several works have studied how the hydrogen bonds, which are between water molecules and collagen, stabilize the fiber structure.^{8,11,12,14} We highlighted the decrease of all peaks related to proline and hydroxyproline collagen residues in AE skin. This observation agrees with previous studies.^{3,6} Using a biochemical method, Smith et al³¹ observed a reduced amount of proline and hydroxyproline in the insoluble collagen fraction of actinic elastosis. Shuster et al³ observed, also using a biochemical approach, a decreased collagen density with aging. Nguyen et al¹⁰ did not observe any variation among subjects of different ages, probably due to the small sample size. In the present study, the decrease of proline and hydroxyproline content in reticular dermis of photoaged skin was clearly measured with Raman spectroscopy.

Raman imaging is a biophysical method well adapted to the analysis of skin samples. This is a technique with strong innovation potential in medical diagnosis and in particular in the field of oncology and dermatology.^{32,33} Here, Raman spectroscopy allowed us to identify molecular markers and organizational states associated with chronological and photoinduced skin aging.

We showed that chronological and photoinduced aging modified both collagen structure and the dermis hydration state. Chronological aging altered in particular the collagen of the papillary dermis while photoaging caused a decrease of collagen stability by altering proline and hydroxyproline residues in the reticular dermis.

CONFLICT OF INTEREST

No conflict of interest to declare.

ORCID

Aurélien Villaret  <http://orcid.org/0000-0003-1242-7717>

Céline Mias  <http://orcid.org/0000-0001-8055-8255>

Valérie Samouillan  <http://orcid.org/0000-0003-0571-3985>

Gwendal Josse  <http://orcid.org/0000-0003-3375-5226>

REFERENCES

- Rittié L, Fisher GJ. Natural and sun-induced aging of human skin. *Cold Spring Harb Perspect Med*. 2015;5(1):a015370.
- Tang R, Samouillan V, Dandurand J, et al. Identification of ageing biomarkers in human dermis biopsies by thermal analysis (DSC) combined with Fourier transform infrared spectroscopy (FTIR/ATR). *Skin Res Technol*. 2017;23:573-580.
- Shuster S, Black MM, McVitie E. The influence of age and sex on skin thickness, skin collagen and density. *Br J Dermatol*. 1975;93:639-643.
- Varani J, Dame MK, Rittie L, et al. Decreased collagen production in chronologically aged skin. *Am J Pathol*. 2006;168:1861-1868.
- Quan T, Fisher GJ. Role of age-associated alterations of the dermal extracellular matrix microenvironment in human skin aging: a mini-review. *Gerontology*. 2015;61(5):427-434.
- Uitto J. Connective tissue biochemistry of the aging dermis. Age-associated alterations in collagen and elastin. *Clin Geriatr Med*. 1989;5:127-147.
- Bernstein EF, et al. Chronic sun exposure alters both the content and distribution of dermal glycosaminoglycans. *Br J Dermatol*. 1996;135(2):255-262.
- Lee DH, Oh JH, Chung JH. Glycosaminoglycan and proteoglycan in skin aging. *J Dermatol Sci*. 2016;83(3):174-181.
- Zhang Q, Andrew Chan KL, Zhang G, et al. Raman microspectroscopic and dynamic vapor sorption characterization of hydration in collagen and dermal tissue. *Biopolymers*. 2011;95(9):607-615.
- Nguyen TT, Happillon T, Feru J, et al. Raman comparison of skin dermis of different ages: focus on spectral markers of collagen hydration. *J Raman Spectrosc*. 2013;44(9):1230-1237.
- Bella J, Eaton M, Brodsky B, Berman H. Crystal and molecular structure of a collagen-like peptide at 1.9 Å resolution. *Science*. 1994;266(5182):75-81.
- Bella J, Brodsky B, Berman HM. Hydration structure of a collagen peptide. *Structure*. 1995;3(9):893-906.
- Gniadecka M, Faurskov Nielsen O, Christensen DH, Wulf HC. Structure of water, proteins, and lipids in intact human skin, hair, and nail. *J Invest Dermatol*. 1998;110(4):393-398.
- Gniadecka M, Nielsen OF, Wessel S, Heidenheim M, Christensen DH, Wulf HC. Water and protein structure in photoaged and chronically aged skin. *J Invest Dermatol*. 1998;111(6):1129-1133.
- Nakagawa N, Matsumoto M, Sakai S. In vivo measurement of the water content in the dermis by confocal Raman spectroscopy. *Skin Res Technol*. 2010;16(2):137-141.
- Frushour BG, Koenig JL. Raman scattering of collagen, gelatin, and elastin. *Biopolymers*. 1975;14(2):379-391.
- Ikoma T, Kobayashi H, Tanaka J, Walsh D, Mann S. Physical properties of type I collagen extracted from fish scales of *Pagrus major* and *Oreochromis niloticus*. *Int J Biol Macromol*. 2003;32(3-5):199-204.
- Nguyen TT, Gobinet C, Feru J, et al. Characterization of Type I and IV collagens by Raman microspectroscopy: identification of spectral markers of the dermo-epidermal junction. *Spectroscopy*. 2012;27:421-427.
- de Vasconcelos Nasser Caetano L, de Oliveira Mendes T, Bagatin E, et al. In vivo confocal Raman spectroscopy for intrinsic aging and photoaging assessment. *J Dermatol Sci*. 2017;88(2):199-206.
- González FJ, Castillo-Martínez C, Martínez-Escanamé M, et al. Noninvasive estimation of chronological and photoinduced skin damage using Raman spectroscopy and principal component analysis. *Skin Res Technol*. 2011;18:442-446.
- Vierkötter A, Ranft U, Krämer U, Sugiri D, Reimann V, Krutmann J. The SCINEXA: a novel, validated score to simultaneously assess and differentiate between intrinsic and extrinsic skin ageing. *J Dermatol Sci*. 2009;53(3):207-211.
- Mainreck N, Brézillon S, Sockalingum GD, Maquart FX, Manfait M, Wegrowski Y. Rapid characterization of glycosaminoglycans using a combined approach by infrared and Raman microspectroscopies. *J Pharm Sci*. 2011;100(2):441-450.
- Yaowu X, Mingsheng G, Peng Z, et al. Wavelength-dependent conformational changes in collagen after mid-infrared laser ablation of cornea. *Biophys J*. 2008;94(4):1359-1366.

24. Debelle L, Alix AJ, Wei SM, et al. The secondary structure and architecture of human elastin. *Eur J Biochem.* 1998;258(2):533-539.
25. Gkogkolou P, Böhm M. Advanced glycation end products. *Dermatoendocrinol.* 2012;4(3):259-270.
26. Guilbert M, Said G, Happillon T, et al. Probing non-enzymatic glycation of type I collagen: a novel approach using Raman and infrared biophotonic methods. *Biochem Biophys Acta.* 2013;1830(6):3525-3531.
27. Oh JH, Kim YK, Jung JY, et al. Intrinsic aging- and photoaging-dependent level changes of glycosaminoglycans and their correlation with water content in human skin. *J Dermatol Sci.* 2011;62(3):192-201.
28. Nguyen TT, Eklouh-Molinier C, Sebiskveradze D, et al. Changes of skin collagen orientation associated with chronological aging as probed by polarized-FTIR micro-imaging. *Analyst.* 2014;139(10):2482-2488.
29. Ly E, Piot O, Durlach A, Bernard P, Manfait M. Polarized Raman microspectroscopy can reveal structural changes of peritumoral dermis in basal cell carcinoma. *Appl Spectrosc.* 2008;62(10):1088-1094.
30. Short MA, Lui H, McLean D, Zeng H, Alajlan A, Chen XK. Changes in nuclei and peritumoral collagen within nodular basal cell carcinomas via confocal micro-Raman spectroscopy. *J Biomed Opt.* 2006;11(3):34004.
31. Smith JG Jr, Davidson EA, Sams WM Jr, Clark RD. Alterations in human dermal connective tissue with age and chronic sun damage. *J Invest Dermatol.* 1962;39(4):347-350.
32. Janssens M, van Smeden J, Puppels GJ, Lavrijsen AP, Caspers PJ, Bouwstra JA. Lipid to protein ratio plays an important role in the skin barrier function of atopic eczema patients. *Br J Dermatol.* 2014;170:1248-1255.
33. Piredda P, Berning M, Boukamp P, Volkmer A. subcellular Raman microspectroscopy imaging of nucleic acids and tryptophan for distinction of normal human skin cells and tumorigenic keratinocytes. *Anal Chem.* 2015;87:6778-6785.

How to cite this article: Villaret A, Ipinazar C, Satar T, et al. Raman characterization of human skin aging. *Skin Res Technol.* 2018;00:1-7. <https://doi.org/10.1111/srt.12643>